



Atmospheric and kinetic studies of OH and HO₂ by the FAGE technique

D. Amedro^{1,2}, K. Miyazaki^{1,2}, A. Parker¹, C. Schoemaeker^{1,*}, C. Fittschen¹

1. Laboratoire PC2A, Université de Lille 1- Bâtiment C11, 59655 Villeneuve d'Ascq, France. E-mail: Coralie.Schoemaeker@univ-lille1.fr
2. Department of Applied Chemistry, Tokyo Metropolitan University, Japan

Abstract

A new FAGE setup has recently been built at the University of Lille, France. It permits the quantification of OH and HO₂ in the atmosphere with a detection limit of 3×10^5 molecules/(cm³·min) for OH and 1×10^6 molecules/(cm³·min) for HO₂. Its coupling to a photolysis cell enables the measurement of the total reactivity of the hydroxyl radical in ambient air and kinetic studies in laboratory. Two configurations have been considered: one with the photolysis cell at 90° to the FAGE nozzle, the other on line with the FAGE nozzle. The two configurations have been tested and validated by measuring the well known rate constants of OH with CH₄, C₃H₈ and CO. The advantages and drawbacks of each configuration have been evaluated. The “on line” configuration limits losses and permits measurements over a larger reactivity range but is affected by OH formation from the laser beam striking the FAGE nozzle, thus limiting the ability to carry out energy dependence studies which can, in contrast, be successfully performed in the 90° configuration.

Key words: OH; kinetic; reactivity; laser induced fluorescence

DOI: 10.1016/S1001-0742(11)60723-7

Introduction

OH is the principle atmospheric oxidant and is at the origin of the majority of chemical transformations in the atmosphere (Finlayson-Pitts and Pitts, 1986). The chemical mechanisms leading to its formation and consumption are very complex and understanding of different pathways is key to the ability to accurately model atmospheric chemistry and to predict atmosphere evolution. In order to study the OH production and loss, techniques for the field measurements of absolute concentrations of OH and HO₂ have been developed over the past two decades. Indeed, as OH is highly reactive (atmospheric lifetime in the range of the ms), strongly linked to the photochemistry, and as its concentration and temporal variation are very sensitive to environmental changes, comparison between experimental measurements and models can allow the evaluation of the quality of the chemical mechanisms present in the models and the level of knowledge of the chemistry at the site considered.

Different techniques, reviewed by Heard and Pilling (2003), have been used to quantify OH in the atmosphere, species particularly difficult to measure due to its high reactivity and low concentration (10^5 – 10^6 mol/cm³). Of these only a few combine a high detection limit with high temporal and spatial resolutions. The most commonly used technique for field measurements is called FAGE (Fluorescence Array by Gas Expansion). It was pioneered by Hard et al. (1984) in the 1980s, and was based on the detection of OH radicals by laser induced fluorescence

(LIF) at 282 nm after expansion of the sample gas through a pinhole into a low-pressure detection cell to achieve a good enough signal to noise ratio to detect OH in the concentration range found in the atmosphere.

From there, improvements of the technique to limit OH generation by the LIF laser, working at a longer excitation wavelength (308 nm) (Mather et al., 1997), development of new instruments (Holland et al., 1995; Creasey et al., 1997; Kanaya et al., 2001; Dusanter et al., 2009), calibration studies (Bloss et al., 2004; Faloon et al., 2004; Dusanter et al., 2008), adaptation to other species (HO₂: Mather et al., 1997; NO and IO: Bloss et al., 2003; N₂O₅: Matsumoto et al., 2005; RO₂: Fuchs et al., 2008), interference studies (Ren et al., 2004; Fuchs et al., 2011) and intercomparisons between FAGE instruments or with other techniques have all been performed (Campbell et al., 1995; Schlosser et al., 2009; Fuchs et al., 2010).

In parallel, both ground and air based field campaigns have been carried out in many different environments such as: urban (in New York: Ren et al., 2003; in Mexico: Dusanter et al., 2009), clean coastal sites (CHABLIS Bloss et al., 2007; Rishiri Island: Kanaya et al., 2007), rural polluted areas (BERLIOZ: Holland et al., 2003; PRIDE: Lu et al., 2011), coniferous or deciduous forests (Creasey et al., 2001; Dlugi et al., 2010), pristine tropical forests (GABRIEL campaign: Martinez et al., 2010; OP3: Whalley et al., 2011). Systematic differences between the measured and modelled OH concentration profiles have been observed, highlighting missing knowledge in the chemical mechanisms used. In very clean environments these disagreements are often an overestimation of the OH

* Corresponding author. E-mail: Coralie.Schoemaeker@univ-lille1.fr

jesc.ac.cn

and HO₂ concentrations by the model (Bloss et al., 2010) suggesting that important sinks are not taken into account. In contrast, at “polluted” sites (Ren et al., 2006) or in tropical forests (Kubistin et al., 2010), the models often underestimate the measured OH. In forest, this is possibly linked to the chemistry of secondary organic products from biogenic oxidation which plays an important role (Butler et al., 2008; Lelieveld et al., 2008). The identification and quantification of these species is particularly problematic as the type of molecule and the concentrations are unknown and maybe incompatible with detection by the common analytical techniques used to measure VOCs (GC-MS: Lewis et al., 2000; PTR-MS: DeGouw and Warneke, 2007).

Another point of view can be then considered to estimate the effect of the unknown species: the measurement of the total OH reactivity. This measurement provides the lifetime of OH radicals in the presence of the reactive species present in ambient air, and when compared to a reactivity calculated from the concentration of species measured and their rate constants for reaction with OH enables the determination of the extent of the missing species.

In the last decade, new instruments have been developed to measure OH reactivity in the atmosphere. Three principle techniques have been used. The comparative reactivity technique is based on the coupling of a reactor with a PTR-MS. A reference compound and an ambient air sample are introduced into the reactor, where OH is continuously generated. The OH reacts competitively with both the reference compound and species present in the air sample. The concentration of the reference species is followed by the PTR-MS and the change in concentration can be used to calculate the reactivity towards OH of the air (Sinha et al., 2008). The two other techniques both employ FAGE for detecting OH radicals. One uses a continuous generation of OH in a movable injector within a flow tube (Kovacs and Brune, 2001) connected to a FAGE instrument where the OH concentration can be continuously measured as a function of the distance of the injector from the measurement region. In the other technique, a laser photolyses ozone in the UV in the presence of ambient water vapour to form a pulse of OH radicals, the decay of this OH pulse being observed through time resolved measurements with a FAGE (Sadanaga et al., 2004).

Both techniques have been deployed in field campaigns for ground based measurements (Harder and Pilling, 2003; Carlo et al., 2004; Yoshino et al., 2006; Lou et al., 2010).

Recently, a few fields campaigns have combined the quantification of OH and HO₂ with reactivity measurements (INTEX B, airborne measurements: Mao et al., 2009; PRIDE, ground field campaign: Lu et al., 2011), which greatly improves the possibility of fully characterising the oxidative capacity at a specific site, but requires the simultaneous employment of two dedicated complex and expensive instruments.

At the University of Lille 1, a new FAGE setup (UL-FAGE) has recently been developed for the measurement of OH and HO₂ in the atmosphere during field campaigns.

When coupled to an atmospheric temperature and pressure laser photolysis cell, it can be applied to kinetic studies in laboratory or to the total OH reactivity measurements in ambient air.

This article describes the UL-FAGE and its coupling to two photolysis cells: one “on line” and the other at 90° to the measurement axis, including the validation of these cells by measuring the well known rate constants of the CH₄, C₃H₈ and CO + OH reactions. The advantages and drawbacks of each configuration have been evaluated.

1 Description of experimental technique

1.1 FAGE instrument

The newly developed University of Lille Fluorescence Assay by Gas Expansion (UL-FAGE) instrument shown in Fig. 1 has been detailed previously (Parker et al., 2011). It consists of two White type multipass cells similar to those used at Pennsylvania State University (Faloona et al., 2004) (aligned to give approximately 30 passes) mounted in series to detect OH and HO₂ simultaneously. In the first cell OH is measured by LIF, while in the second HO₂ is measured indirectly by injecting NO to convert the HO₂ to OH which is subsequently detected by LIF. Our FAGE setup continuously pumps the ambient air through a small aperture (1 mm) into the low pressure cells (1.5 Torr) at a flow rate of 9.2 L/min with an Edwards GX6/100L pump.

The LIF signal is generated by exciting OH molecules (A-X 0-0, Q₁(3) at 308.244 nm) using a frequency doubled dye laser (Sirah Laser PrecisionScan PRSC-24-HPR) pumped by the frequency doubled output of a Nd:YVO₄ laser (Spectra Physics Navigator II YHP40-532QW), working at a repetition rate of 5 kHz. The laser energy is split between the OH cell (2 mW), the HO₂ cell (1 mW) and the wavelength reference cell (0.3 mW) using CVI Melles Griot beam splitters, the OH and HO₂ beams being coupled to two 10 m OZ Optics fibres of 200 μm diameter via collimators (Melles Griot) for transport to the detection cells. The transmission through the 10 m fibre is roughly 65%. However, the major losses occur when coupling the light into the fibres and depend critically on the alignment: between 15% and 20% of the initial dye laser output (around 15 mW) reach the OH cell and 5% to 10% reach the HO₂ cell.

As under atmospheric conditions the HO₂ concentration

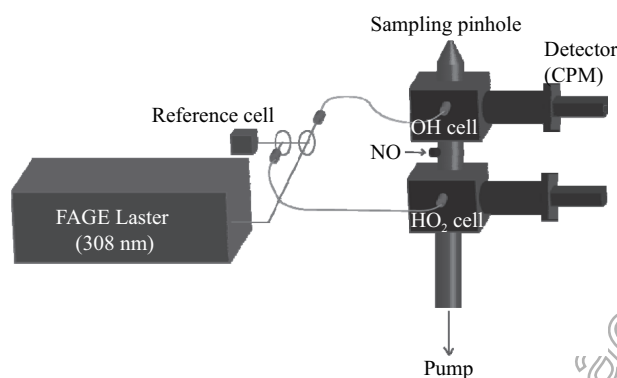


Fig. 1 FAGE instrument scheme.

is approximately two orders of magnitude higher than OH, more power is injected into the OH cell to increase the sensitivity of the OH quantification, which owing to the lower concentration is more critical than the sensitivity of the HO₂ measurement. In order to stabilize the emission of the fluorescence excitation laser, a constant OH radical concentration is generated in the reference cell by water vapour thermolysis and the ensuing fluorescence intensity following excitation is continuously measured. A decrease in the signal engenders an automatic wavelength scan through a Labview program.

The resulting LIF signal from the excited OH, also at 308 nm (A-X 0-0), is detected perpendicular to the excitation beam after passing through two focusing lenses and an interference filter (Barr Associates). Care has been taken to reduce the stray light as much as possible by installing several baffles within the cell to remove extraneous light; in addition the inner surfaces of the cell are black and have been machined to be very rough to avoid reflections. The detection is done by photon counting with gated CPM (Channel Photon Multiplier, Perkin-Elmer MP-1982) modules connected to a counting card (National Instruments PCI-6602) installed in a PC. The low pressure in the FAGE cells, which reduces collisional quenching and therefore prolongs the fluorescence lifetime, makes it possible to separate the stray light from the excitation laser pulse and the fluorescence signal by way of temporal discrimination.

Fluorescence is then collected from 400 to 1200 nsec after the laser pulse, which corresponds to the time between turning on the detector and the fluorescence intensity becoming too low to be advantageously collected, i.e., a longer measurement time would not increase the signal-to-noise ratio anymore.

Before each FAGE cell a perforated loop of 1/8th inch Teflon tubing has been installed through which additional reagents can be added. HO₂ is measured in the second cell in this way by adding a small flow of pure NO (99.9%, air liquide) which converts most HO₂ radicals to OH radicals in a rapid reaction. OH is then measured by LIF. To obtain the “real” HO₂ concentration, the residual OH signal, calculated from the signal in the first cell weighted by the relative sensitivities of the cells determined by separate calibration, is subtracted.

1.2 Use in the quantification mode

This setup can be used to measure atmospheric OH and HO₂ during field campaigns, as it has an excellent OH detection limit of 3×10^5 mol/cm³ for an average time of 1 min.

The HO₂ detection limit can in theory be the same but because the laser power used in the HO₂ cell is lower than in the OH cell, the resulting detection limit for HO₂ is 1×10^6 mol/cm³ in 1 min. These detection limits are given for a signal/noise ratio of 1 using the calibration of the instrument.

Indeed, as it is very difficult to calculate the absolute concentration directly from the fluorescence signal, a calibration is necessary. This is done by placing a calibration cell on top of the FAGE inlet nozzle. In the calibration cell,

a known concentration of water vapour is photolysed at 184.9 nm by a mercury lamp thus generating a low, known concentration of OH and HO₂.



The OH concentration generated can be calculated:

$$[\text{OH}] = [\text{HO}_2] = F_{184.9} \times \sigma_{\text{H}_2\text{O}} \times [\text{H}_2\text{O}] \times \phi \times \Delta t \quad (3)$$

where, $\sigma_{\text{H}_2\text{O}}$ (Cantrell et al., 1997) and ϕ (Atkinson et al., 2004) are known and [H₂O] is measured accurately by a dew point hygrometer. The lamp flux: $F_{184.9}$ is measured indirectly by actinometry by simultaneously measuring the O₃, produced by photolysis of O₂ at 184.9 nm, with a commercial analyser (TEI 49i). OH_{losses} are the OH losses between the OH generation point and the nozzle and is determined by changing the position of the lamp along the calibration cell.

The calibrations are performed with a turbulent flow of 40 L/min in the calibration cell with a water concentration in the range of 1000–3000 ppm leading to an OH and HO₂ production of 10^8 – 10^9 mol/cm³.

Because the FAGE instrument is composed of two cells, different parameters have to be determined for each cell during the calibration process. The calibration factor (in counts·sec⁻¹·molecule⁻¹·cm³·mW⁻¹) for OH is calculated for cell 1 (OH cell) from the measurement of the signal at a known concentration of OH and a known laser power. As the calibration is carried out in the same conditions as measurements in the atmosphere, the OH losses between sampling and detection in cell 1 are included in the calibration factor as it is the OH concentration present at the entrance of the nozzle which is considered in the calculation.

In cell 2 (HO₂ cell), the calibration is performed under two different conditions: with and without NO. Without NO, the calibration factor for OH is measured. In the same way as in the first cell, the OH losses between the cone and the detection region in cell 2 are included in this factor. With NO, as the HO₂ has been converted in OH, the measured signal originates from both OH and HO₂. The signal from OH is known and corresponds to the signal measured without NO and can then be subtracted from the total signal to obtain the HO₂ calibration factor (in counts·sec⁻¹·mol⁻¹·cm³·mW⁻¹).

It should be noted that we assume no losses of HO₂ between the inlet nozzle and the detection region in cell 2. This assumption is reliable because of the low reactivity of HO₂ compared to OH.

During atmospheric measurements, signals in cells 1 and 2 are measured simultaneously. The measurements in cell 1 provide the OH concentration, which is used to calculate the contribution of OH in cell 2. As OH

concentrations are usually very low compared to HO₂, this contribution is weak.

OH and HO₂ measurements in the atmosphere are recorded using the following procedure: the excitation laser is scanned to find the peak of the OH transition and the fluorescence signal in the reference cell at the peak is recorded. The laser is then set to the peak of the OH transition for 20 sec and the signal summed during that time. The wavelength is then shifted by 0.02 nm to a wavelength where OH is not excited to measure the background due to laser and solar radiation. It then takes a further 20 sec to return to the peak by a step by step process whereby Labview steps the laser wavelength while monitoring the effect on the LIF signal in the reference cell to achieve at least 95% of the signal obtained during the previous scan. If the 95% can not be achieved then a new scan is launched to find the peak again.

An intercomparison campaign was undertaken in the SAPHIR smog chamber in April 2010 in Jülich (Germany), with measurements performed under several different experimental conditions (e.g., ozone, NO_x, humidity). The results show a good correlation with the Jülich FAGE instrument that is permanently installed at the chamber and further details on this intercomparison can be found in the dedicated EUROCHAMP report (Fittschen et al., 2010). In addition, the UL-FAGE participated in the HCCT (Hill Cap Cloud Thuringa) campaign in September 2010. This campaign, following the two previous FEBUKO campaigns (Herrmann et al., 2005) had the aim of better understanding the transformation mechanisms of the gas, liquid and solid phases linked to an air mass passing through a cloud. For that, numerous instruments for the characterisation of these phases were installed at three sites (upwind, in the cloud and downwind), one being on top of a hill where orographic clouds are frequently observed. Among these two FAGE instruments were deployed: the UL-FAGE at the upwind site and the University of Leeds FAGE on top of the hill. Results are under analysis and will be the subject of future publications but the first results showed that the OH concentrations were below our detection limit during the cloud events.

1.3 Use in kinetic/reactivity mode

For kinetic measurements, the FAGE set-up described in Section 1.1 is used to measure the time resolved OH signal from a photolysis cell after its generation by laser photolysis. The FAGE cells are connected to the photolysis cell which has optical access permitting the photolysis of the gas mixture and therefore the generation of radicals at various wavelengths from the UV (266 nm, quadrupled YAG) to the visible (YAG + dye laser), depending on the goal of the study.

Two different cell configurations (Fig. 2) were tested to limit and to better understand the physical processes taking place during the time resolved measurement of OH in the photolysed volume. These processes such as diffusion out of the photolysed volume or losses on the reactor wall, might affect the OH decay time profile. For both configurations, the technique of measuring the OH decay

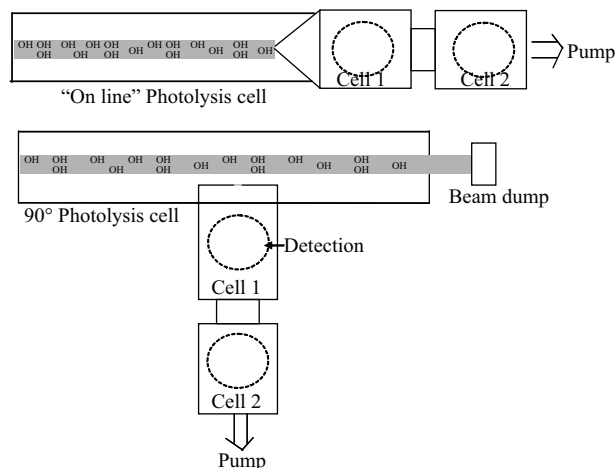


Fig. 2 Kinetic configurations schemes for the laser photolysis cell: upper graph on line configuration (OLC), lower graph 90° configuration (NDC).

(i.e., OH signal as a function of time after photolysis) is the same: instead of summing LIF excitation pulses over a long time period to increase the signal and the sensitivity as is done in quantification mode, the signal is recorded synchronized with the photolysis laser pulse and all fluorescence signals occurring at the same delay with respect to the photolysis laser are summed for several photolysis pulses. As the LIF excitation laser repetition rate is 5 kHz, this results in a time resolution of 200 μ sec.

This mode requires the synchronisation of the fluorescence excitation with the photolysis pulse. This was presented previously (Parker et al., 2011). The synchronisation is achieved with two delay generators (DG535, Stanford research Systems) and the PC counting card *via* LabView (v7.1, National Instruments). Delay generator 1 triggers at 5 kHz the excitation laser, the corresponding fluorescence measurement period and the second delay generator, which in turn triggers the photolysis laser at a repetition rate between 0.1 to 10 Hz (a dummy delay on an unused channel of the delay generator is used to decrease the repetition rate of the photolysis laser). The photolysis laser in turn triggers the start of data acquisition. Data are typically summed over 1000–1500 photolysis laser pulses at 2 Hz repetition rate.

Two different configurations for the photolysis cell are used as shown in Fig 2: in the "on line" configuration (OLC), the photolysis cell is coupled to the FAGE on the pumping axis. This combination is the first in the world and was built to limit physical interferences during the pumping as the photolysis volume is centered on the probing nozzle. As the characterization of the OLC photolysis cell was described previously (Parker et al., 2011), it will be only presented through a comparison with the 90° configuration (NDC).

Both cells are made of aluminium: cylindrical (length: 48 cm, diameter: 5 cm) for the OLC, plane-parallel (length: 100 cm, sides: 6 cm \times 6 cm) for the NDC. The cells are closed on one side by a Suprasil quartz window (CVI Melles Griot) mounted on flanges which allow the photolysis laser beam to enter. In the OLC, the other end is connected to the sampling cone of the FAGE cell. For the NDC, the other end is equipped with a window similar

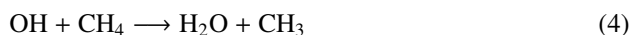
to the first one and a beam dump is used to trap the laser beam. Gases are introduced *via* a Swagelok fitting on one side, further Swagelok fittings are mounted at the other end to allow an extra pump along with additional sampling instruments (O_3 , NO_x , H_2O) as well as pressure/temperature monitoring to be connected. The two configurations are presented schematically in Fig. 2.

2 Validation /comparison of the kinetic configurations

The description and validation of the OLC cell was already presented in a previous study (Parker et al., 2011). A comparison of the two different cells configuration (OLC and NDC) is now given together with the validation of the NDC cell.

2.1 Extraction of kinetic data from measurements in the 90° configuration

OH radicals have been generated in all experiments by the photolysis of O_3 at 282 nm in the presence of H_2O . The NDC cell was validated through the measurement of three well known rate constants:



OH decays have been measured under pseudo first-order conditions, as was previously reported for the OLC cell.

O_3 was produced using an ozone generator (SYCOS KT-GPTM, Ansyco, Germany) and mixed with zero air at low water vapour and CH_4 (or CO , C_3H_8) (N55 for CH_4 , N35 for C_3H_8 and 1% in N_2 for CO both from Air Liquide, France). All experimental conditions are compared with the OLC cell and presented in Table 1. The different gases were introduced to the reactors using calibrated mass flow controllers (F-201, Bronkhorst, The Netherlands and 5800S, Brooks, USA). Pressure within the photolysis cell was kept constant and monitored with a 0–3 bar pressure transmitter (PAA-41, Keller, Switzerland).

Typical OH decays are shown in Fig. 3 for the two different beam shapes, using the same initial O_3 and H_2O concentrations. OH decays obtained for the non-expanded beam for the reaction of $CH_4 + OH$ are presented for three different CH_4 concentrations in Fig. 4.

Experiments have also been performed using two different laser beam sizes, non-expanded and expanded, using the experimental conditions shown in Table 2.

The main difficulty in the determination of the rate constants from the recorded OH decay is to apply a correct fitting procedure for OH signals. It has been shown in our earlier work (Parker et al., 2011) that with the decays

Table 1 Experimental conditions for the different experiments

Parameter	NDC	OLC
p-range (Torr)	760	350–800
Total flow (min^{-1})	20	11.5
Flow through FAGE (min^{-1})	9.2	9.2
$[CH_4]$ range (cm^{-3})	3×10^{15} – 10×10^{15}	3×10^{15} – 30×10^{15}
$[CO]$ range (cm^{-3})	0.7×10^{14} – 3×10^{14}	2×10^{13} – 30×10^{13}
$[C_3H_8]$ range (cm^{-3})	1×10^{13} – 10×10^{13}	–
k'_{max} (sec^{-1})	100	200

Table 2 Experimental conditions for both beam profile

	Expanded	Non-expanded
Laser energy (mJ/cm^2)	1.1	4.5
Beam diameter (cm)	2	1
$[O_3]$ (cm^{-3})	0.2×10^{12} – 2×10^{12}	
$[H_2O]$ (cm^{-3})	0.1×10^{17} – 1×10^{17}	
$[OH]_0$ (cm^{-3})	10^7 – 10^8	10^8 – 10^9

recorded in the OLC cell, the start time of the exponential fit is crucial as the decay is at short reaction time a convolution of the physical increase of OH concentration reaching the detection cell and the chemical consumption in the photolysis cell. In the NDC cell configuration presented in this work, the physical mixing processes are much more complex, as the sampling is not centered on the photolysis volume but is occurring at the border of the photolysed volume, i.e., the laser beam is aligned to be as close as possible to the inlet nozzle without touching it. Therefore, the rise time is longer than in the OLC cell.

To find the best combination of experimental parameter and fitting procedure, various tests have been carried out to optimize the working conditions considering the expected OH decay rates. The rise of the signal has been fitted as a single exponential growth for both, expanded and non-expanded beam, in contrast to our earlier work (Parker et al., 2011). The decay however required two different fitting procedures to best reproduce the expected rate constant: (1) A single exponential decay as used in the OLC configuration was considered for measurements performed in the expanded beam case. (2) A double exponential decay had to be considered for the non-expanded beam, indicating that the decay of OH concentration due to diffusion is the major “loss” reaction at short reaction times. Only at longer reaction times, when OH concentration in the photolysis cell has become more uniform, the decay is mainly due to a loss due to chemical reactions.

Examples for both beam shape are given in Fig. 3. In the case of the non-expanded beam, the first decay (which has already been observed in other instruments (Sadanaga et al., 2005)) is probably mainly due to physical phenomena involving the decrease of the OH concentration due to diffusion of radicals out of the photolysis volume, the second decay is then linked to the OH decay due to the chemical reaction. In the case of the expanded beam, the decay can be well reproduced by a mono-exponential decay, indicating that the diffusion is already advanced at the time, when the signal reaches its maximum and does not markedly influence the OH decay. In the expanded case, the limitation is the low signal/noise ratio achieved

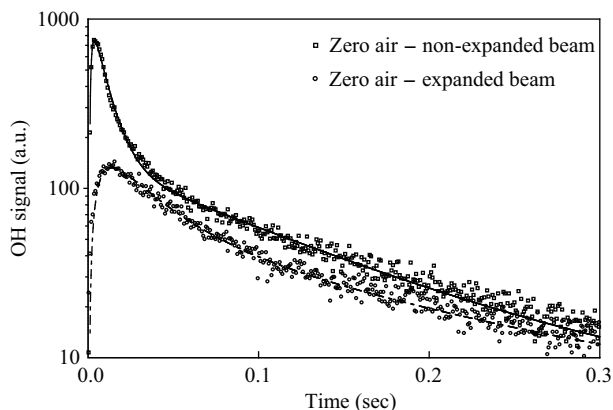


Fig. 3 Comparison between two OH time decay profiles in zero air in the NDC: Non-expanded beam, expanded beam. The solid line corresponds to a fit using a double exponential decay, $k'_0 = 9.72 \text{ sec}^{-1}$. The dashed line represents a fit using a single exponential decay, $k'_0 = 13.86 \text{ sec}^{-1}$.

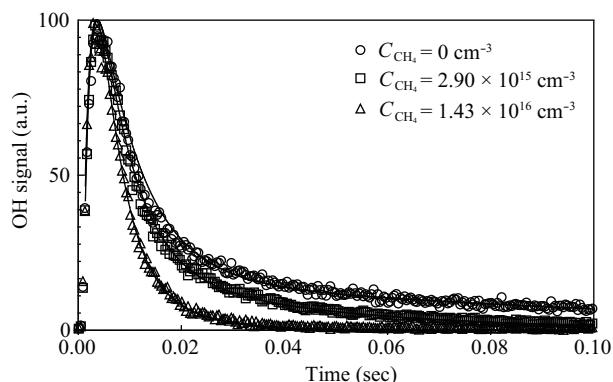


Fig. 4 OH decays for 3 different CH₄ concentrations, obtained in the NDC with non-expanded beam.

which is due to the relatively low energy output of the frequency doubled dye laser used in this study (< 5 mJ/pulse). The use of a more powerful laser, such as a quadrupled YAG laser as used in the OCL configuration (Parker et al., 2011) will provide a better signal to noise ratios.

Different fitting processes were tested to extract the pseudo first-order rate constants from the chemical decays. These rate constants are then plotted against the reactant concentration to determine the rate constant of the reaction (Parker et al., 2011), a typical procedure in kinetic studies. The goal of this work was not to measure again the rate constants for Reactions (4) to (5), but rather use the well known rate constants to extract the most reliable fitting equation for future measurement under different conditions (laboratory kinetic studies or OH lifetime measurements in field studies).

Examples of profiles in zero air as presented in Fig. 3 illustrate very well the differences for the two beam configurations. The rate constants of Reactions (4) to (5) have been measured using different configurations. Table 3 reports the values obtained, compared to those obtained in the OLC.

It can be seen from Table 3 that the rate constant for Reaction (4) has a large scatter between the three different values, and that the non-expanded measurement does not

agree within the error limit with recent recommendations. It must however be pointed out, that the Reaction (4) is very slow, and low concentrations of highly reactive impurities can induce large errors. Reaction (4) also results in slightly too high rate constants for both configurations, NDC and OLC, while the agreement with recent recommendation is very good for Reaction (5).

It is clear, that both expanded and non-expanded beam have some weakpoints, and that the ideal case would be to photolyse the entire volume, i.e., a large expanded beam aligned into the centre of the photolysis cell. The photolysis laser used for this study was not powerful enough to test this configuration, however we have tested the impact of the position of the laser beam with respect to the inlet nozzle on the OH profile. In Fig. 5, two OH decays using the same, non-expanded photolysis beam and the same initial reactant concentration are plotted: the upper black curve has been obtained by aligning the laser beam just above the inlet nozzle, while the lower blue trace has been obtained by aligning the laser 12 mm above the inlet nozzle, i.e., close to the centre of the cell.

The red dashed lines represent a double exponential decay for the 0 mm trace, while a single exponential decay has been used for the 12 mm trace, not taking into account the slow rise. Decay rates of 13.10 and 13.76 sec^{-1} are obtained for the second decay of the 0 mm trace and the single decay of the 12 mm trace respectively. This result is very promising for future experiments, when a more powerful quadrupled YAG laser will be available for photolysis experiments.

A first application of the NDC configuration using a dye laser at 565 nm to excite NO₂ has been done. The aim was the study of the controversial formation of OH radicals by the reaction of NO₂ excited in the visible with water, proposed as a potential new source of OH in the atmosphere (Amedro et al., 2011).

2.2 Comparison of the advantages/drawbacks of the two configurations

The advantages and drawbacks of the OLC can be compared to those of the NDC. (1) The OLC samples from the centre of the photolysed volume, in line with the

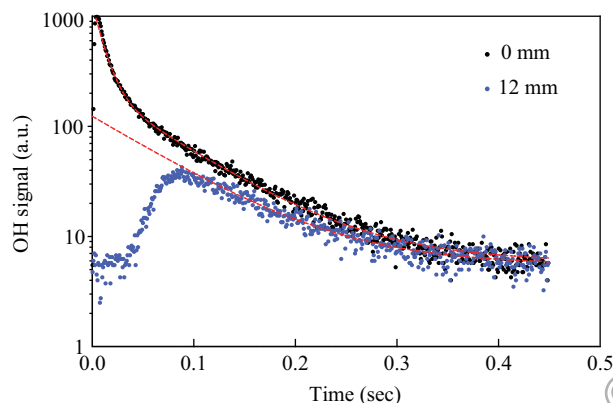


Fig. 5 OH decays obtained by aligning the photolysis laser at two different positions with respect to the inlet nozzle.

Table 3 Rate constants measured in OLC and NDC at 296 K

	k_5 (CH ₄ + OH) (cm ³ /(mol·sec))		k_6 (CO + OH) (cm ³ /(mol·sec))	k_7 (C ₃ H ₈ + OH) (cm ³ /(mol·sec))
	Non expanded	Expanded	Non expanded	Non expanded
NDC	$(7.2 \pm 0.7) \times 10^{-15\#}$	$(5.8 \pm 0.1) \times 10^{-15}$	$(2.7 \pm 0.2) \times 10^{-13}$	1.04×10^{-12}
OLC	$(6.2 \pm 0.2) \times 10^{-15}$		$(2.5 \pm 0.2) \times 10^{-13}$	–
Rec.*	6.01×10^{-15}		2.31×10^{-13}	1.05×10^{-12}

* Recommended rate constants all from Atkinson et al., 2006, all errors are statistical only, except for #: standard deviation of three individual measurements.

macroscopic gas flow direction, therefore decrease the influence of physical effects such as diffusion. As the initial increase in signal is fast but non-exponential, the fitting of the OH decay is started after a fixed delay with respect to the photolysis laser. This delay has been deduced empirically by measuring well-known rate constants (Parker et al., 2011). Decays of up to 200 sec⁻¹ can be measured in this configuration. (2) The NDC samples from the extremity of the photolyzed volume at 90° with respect to the macroscopic gas flow directions. Therefore, in this configuration physical effects such as diffusion and probably turbulences influence the OH profile much more. The rise is slower and exponential and enables the fitting of the complete profile. Depending on the size of the photolyzed volume, either mono- or biexponential decays will be fitted to best reproduce the experimental traces. Decays of up to 100 sec⁻¹ can be measured in this configuration. (3) Even though faster decays can be measured in the NDC configuration, a major drawback of the OLC is that the entire FAGE cells must be rotated by 90° from their quantification configuration, making switching from quantification to reactivity slow and tedious. The NDC does not require this rotation, and therefore a faster change is possible, an important issue during field campaigns.

2.3 Interferences within both configurations

The energy dependence of the OH-fluorescence signal was studied in both configurations. While the OH signal increases linearly with laser energy in the NDC, we observed unexpected OH formation in the OLC: increased concentration of OH were detected when a mixture of He and water was photolysed at 282 nm, as shown in Fig. 6. Also, O₃ and NO_x were detected in the gas mixtures at the exit of the photolysis cell after photolysis of a mixture of air and water at 282 nm, using commercial analyzers (Fig. 7). We suspect this formation to be due to the generation of a plasma when the laser strikes the metallic surface around the FAGE inlet nozzle. Due to this effect this configuration can not be used to study of reactions leading to OH formation such as photolysis reactions. However, these processes are strongly dependant on the laser fluence and kinetic studies can be done at relatively low laser power where the interference is weak and short lived, and does not affect rate constant or reactivity measurements.

The same energy dependence of the signal was tested in the NDC cell: no such unexpected formation of OH radicals or other species has been observed, even at the highest energies.

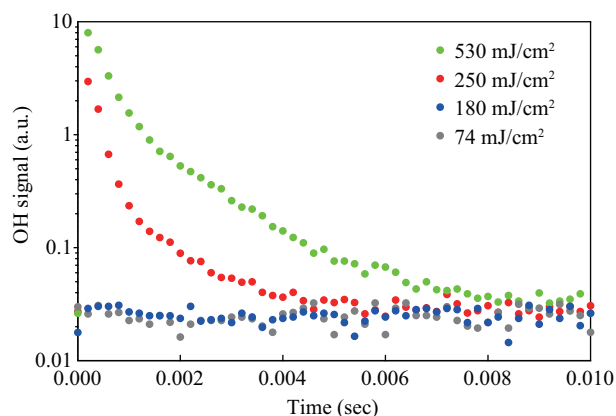


Fig. 6 Interference generation of OH radicals through impact of photolysis laser beam onto the metal nozzle in the OLD configuration.

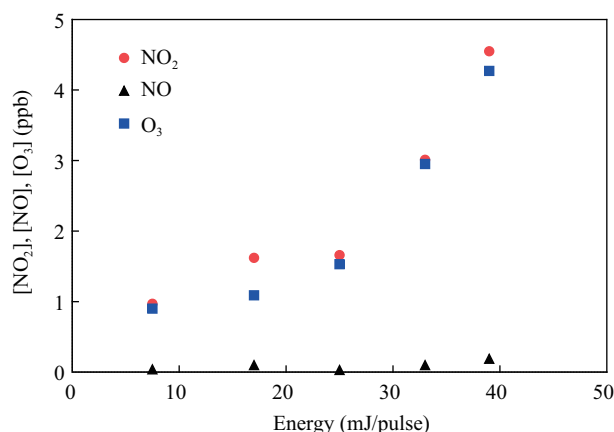


Fig. 7 Interference generation of species in the OLC.

3 Conclusions

This study has shown the potential of the new UL-FAGE for the quantification of OH and HO₂ in the atmosphere as well as its use for kinetic applications when coupled to a photolysis cell. For kinetic applications, two configurations were used: with a photolysis cell “on line” with respect to the gas flow and the FAGE detection and another one with the FAGE at 90° with respect to the gas flow. The use of the two configurations for rate constant measurements involving OH consumption were validated through the measurement of known rate constants. Different fitting procedures needed to be applied, adapted to the different configurations.

The limitation and advantages of both configurations were discussed: the “on line” configuration allows for the measurement of faster decays, but can not be used for OH

formation and energy dependence studies due to interferences probably from the laser beam hitting a metal surface. Both configurations can be used for kinetic laboratory studies and reactivity measurements in the atmosphere, however the 90° configuration is easier to adapt from the quantification to the reactivity mode.

Acknowledgments

This work is jointly supported by the Nord-Pas de Calais region in the frame of the IRENI research program, by the French Research Ministry, by the European Fund for Regional Economic Development (FEDER). A. Parker thanks the EU for financial support through project MEST-CT-2005-020659. K. Miyazaki thanks the French Government for financial aid through an EIFFEL scholarship.

References

- Amedro D, Parker A E, Schoemaeker C, Fittschen C, 2011. Direct observation of OH radicals after 565 nm multiphoton excitation of NO₂ in the presence of H₂O. *Chemical Physics Letters*, 513(1-3): 12–16.
- Atkinson R, Baulch D L, Cox R A, Crowley J N, Hampson R F, Hynes R G et al., 2004. Evaluated kinetic and photochemical data for atmospheric chemistry: volume 1 – gas phase reactions of Ox, HOx, NOx, and SOx, species. *Atmospheric Chemistry and Physics*, 4(6): 1461–1738.
- Atkinson R, Baulch D L, Cox R A, Crowley J N, Hampson R F, Hynes R G et al., 2006. Evaluated kinetic and photochemical data for atmospheric chemistry: Volume II – gas phase reactions of organic species. *Atmospheric Chemistry and Physics*, 6(11): 3625–4055.
- Bloss W J, Camredon M, Lee J D, Heard D E, Plane J M C, Saiz-Lopez A et al., 2010. Coupling of HOx, NOx and halogen chemistry in the antarctic boundary layer. *Atmospheric Chemistry and Physics*, 10(21): 10187–10209.
- Bloss W J, Gravestock T J, Heard D E, Ingham T, Johnson G P, Lee J D, 2003. Application of a compact all solid-state laser system to the in situ detection of atmospheric OH, HO₂, NO and IO by laser-induced fluorescence. *Journal of Environmental Monitoring*, 5(1): 21–28.
- Bloss W J, Lee J D, Bloss C, Heard D E, Pilling M J, Wirtz K et al., 2004. Validation of the calibration of a laser-induced fluorescence instrument for the measurement of OH radicals in the atmosphere. *Atmospheric Chemistry and Physics Discussions*, 4(2): 571–583.
- Bloss W J, Lee J D, Heard D E, Salmon R A, Bauguitte S J B, Roscoe H K et al., 2007. Observations of OH and HO₂ radicals in coastal Antarctica. *Atmospheric Chemistry and Physics*, 7(16): 4171–4185.
- Butler T M, Taraborrelli D, Brühl C, Fischer H, Harder H, Martinez M et al., 2008. Improved simulation of isoprene oxidation chemistry with the ECHAM5/MESy chemistry-climate model: lessons from the GABRIEL airborne field campaign. *Atmospheric Chemistry and Physics*, 8(16): 4529–4546.
- Campbell M J, Hall B D, Sheppard J C, Utley P L, O'Brien R J, Hard T M et al., 1995. Intercomparison of local hydroxyl measurements by radiocarbon and FAGE techniques. *Journal of the Atmospheric Sciences*, 52(19): 3421–3428.
- Cantrell C A, Zimmer A, Tyndall G S, 1997. Absorption cross sections for water vapor from 183 to 193 nm. *Geophysical Research Letters*, 24(17): 2195–2198.
- Creasey D J, Halford-Maw P A, Heard D E, Pilling M J, Withaker B J, 1997. Implementation and initial deployment of a field instrument for measurement of OH and HO₂ in the troposphere by laser-induced fluorescence. *Journal of Chemical Society, Faraday Transaction*, 93(16): 2907–2913.
- Creasey D J, Heard D E, Lee J D, 2001. OH and HO₂ measurements in a forested region of north-western Greece. *Atmospheric Environment*, 35(27): 4713–4724.
- De Gouw J, Warneke C, 2007. Measurements of volatile organic compounds in the earth's atmosphere using proton-transfer-reaction mass spectrometry. *Mass Spectrometry Reviews*, 26(2): 223–257.
- Di Carlo P, Brune W H, Martinez M, Harder H, Leshner R, Ren X R et al., 2004. Missing OH reactivity in a forest: Evidence for unknown reactive biogenic VOCs. *Science*, 304(5671): 722–725.
- Dlugi R, Berger M, Zelger M, Hofzumahaus A, Siese M, Holland F et al., 2010. Turbulent exchange and segregation of HOx radicals and volatile organic compounds above a deciduous forest. *Atmospheric Chemistry and Physics*, 10(13): 6215–6235.
- Dusanter S, Vimal D, Stevens P S, 2008. Technical note: Measuring tropospheric OH and HO₂ by laser-induced fluorescence at low pressure. A comparison of calibration techniques. *Atmospheric Chemistry and Physics*, 8(2): 321–340.
- Dusanter S, Vimal D, Stevens P S, Volkamer R, Molina L T, 2009. Measurements of OH and HO₂ concentrations during the MCMA-2006 field campaign – Part 1: Deployment of the Indiana University laser-induced fluorescence instrument. *Atmospheric Chemistry and Physics*, 9(5): 1665–1685.
- Faloon I C, Tan D, Leshner R L, Hazen N L, Frame C L, Simpas J B et al., 2004. A laser-induced fluorescence instrument for detecting tropospheric OH and HO₂: Characteristics and Calibration. *Journal of Atmospheric Chemistry*, 47(2): 139–167.
- Finlayson-Pitts B J, Pitts J N Jr, 1986. *Atmospheric Chemistry: Fundamentals and Experimental Techniques*. John Wiley and Sons, New York. ISBN 9780471882275.
- Fittschen C, Parker A, Amedro D, Schoemaeker C, Bohn B, Fuchs H, 2010. http://www2.fz-juelich.de/icg/icg-2/eurochamp_php_skripte/eurochamp/pdfs/E2-2010-02-02-0016_report.pdf.
- Fuchs H, Bohn B, Hofzumahaus A, Holland F, Lu K D, Nehr S et al., 2011. Detection of HO₂ by laser-induced fluorescence: calibration and interferences from RO₂ radicals. *Atmospheric Measurement Techniques*, 4(6): 1209–1225.
- Fuchs H, Brauers T, Dorn H P, Harder H, Häsel R, Hofzumahaus A et al., 2010. Technical Note: Formal blind intercomparison of HO₂ measurements in the atmosphere simulation chamber SAPHIR during the HOx Comp campaign. *Atmospheric Chemistry and Physics*, 10(24): 12233–12250.
- Fuchs H, Holland F, Hofzumahaus A, 2008. Measurement of tropospheric RO₂ and HO₂ radicals by a laser-induced fluorescence instrument. *Review of Scientific Instruments*, 79(8): 084104–084112.
- Hard T M, O'Brien R J, Can C Y, Mehrabzadeh A A, 1984. Tropospheric free radical determination by FAGE. *Environmental Science and Technology*, 18(18): 768–777.
- Heard D E, Pilling M J, 2003. Measurement of OH and HO₂ in the troposphere. *Chemical Review*, 103(12): 5163–5198.
- Herrmann H, Wolke R, Müller K, Brüggemann E, Gnauk T, Barzagli P et al., 2005. FEBUKO and MODMEP: Field measurements and modelling of aerosol and cloud mul-

- tiphase processes. *Atmospheric Environment*, 39(23-24): 4169–4183.
- Holland F, Hessling M, Hofzumahaus A, 1995. *In situ* measurement of tropospheric OH radicals by laser-induced fluorescence-A description of the KFA instrument. *Journal of the Atmospheric Sciences*, 52(19): 3393–3401.
- Holland F, Hofzumahaus A, Schäfer J, Kraus A, Pätz H W, 2003. Measurements of OH and HO₂ radical concentrations and photolysis frequencies during BERLIOZ. *Journal of Geophysical Research*, 108(D4): 8246.
- Kanaya Y, Cao R Q, Kato S, Miyakawa Y, Kajii Y, Tanimoto H et al., 2007. Chemistry of OH and HO₂ radicals observed at Rishiri Island, Japan, in September 2003: Missing daytime sink of HO₂ and positive nighttime correlations with monoterpenes. *Journal of Geophysical Research*, 112: D11308.
- Kanaya Y, Sadanaga Y, Hirokawa J, Kajii Y, Akimoto H, 2001. Development of a ground-based LIF instrument for measuring HO_x radicals: Instrumentation and calibrations. *Journal of Atmospheric Chemistry*, 38(1): 73–110.
- Kovacs T A, Brune W H, 2001. Total OH loss rate measurement. *Journal of Atmospheric Chemistry*, 39(2): 105–122.
- Kubistin D, Harder H, Martinez M, Rudolf M, Sander R, Bozem H et al., 2010. Hydroxyl radicals in the tropical troposphere over the Suriname rainforest: comparison of measurements with the box model MECCA. *Atmospheric Chemistry and Physics*, 10(19): 9705–9728.
- Lelieveld J, Butler T M, Crowley J N, Dillon T J, Fischer H, Ganzeveld L et al., 2008. Atmospheric oxidation capacity sustained by a tropical forest. *Nature*, 452(7188): 737–740.
- Lewis A C, Carslaw N, Marriott P J, Kinghorn R M, Morrison P, Lee A L et al., 2000. A larger pool of ozone-forming carbon compounds in urban atmospheres. *Nature*, 405(6788): 778–781.
- Lou S, Holland F, Rohrer F, Lu K, Bohn B, Brauers T et al., 2010. Atmospheric OH reactivities in the Pearl River Delta – China in summer 2006: measurement and model results. *Atmospheric Chemistry and Physics*, 10(22): 11243–11260.
- Lu K D, Rohrer F, Holland F, Fuchs H, Bohn B, Brauers T et al., 2011. Observation and modelling of OH and HO₂ concentrations in the Pearl River Delta 2006: a missing OH source in a VOC rich atmosphere. *Atmospheric Chemistry and Physics Discussions*, 11(4): 11311–11378.
- Mao J, Ren X, Brune W H, Olson J R, Crawford J H, Fried A et al., 2009. Airborne measurement of OH reactivity during INTEX-B. *Atmospheric Chemistry and Physics*, 9(1): 163–173.
- Martinez M, Harder H, Kubistin D, Rudolf M, Bozem H, Eerdeken G et al., 2010. Hydroxyl radicals in the tropical troposphere over the Suriname rainforest: airborne measurements. *Atmospheric Chemistry and Physics*, 10(8): 3759–3773.
- Mather J H, Stevens P S, Brune W H, 1997. OH and HO₂ measurements using laser-induced fluorescence. *Journal of Geophysical Research*, 102(5): 6427–6436.
- Matsumoto J, Imai H, Kosugi N, Kajii Y, 2005. *In situ* measurement of N₂O₅ in the urban atmosphere by thermal decomposition/laser-induced fluorescence technique. *Atmospheric Environment*, 39(36): 6802–6811.
- Parker A E, Amédéo D, Schoemaeker C, Fittschen C, 2011. OH radical reactivity measurements by FAGE. *Environmental Engineering and Management Journal*, 10(1): 107–114.
- Ren X R, Brune W H, Mao J Q, Mitchell M J, Leshner R L, Simpas J B et al., 2006. Behavior of OH and HO₂ in the winter atmosphere in New York City. *Atmospheric Environment*, 40(Suppl. 2): 252–263.
- Ren X R, Harder H, Martinez M, Faloon I C, Tan D, Leshner R L et al., 2004. Interference testing for atmospheric HO_x measurements by laser-induced fluorescence. *Journal of Atmospheric Chemistry*, 47(2): 169–190.
- Ren X R, Harder H, Martinez M, Leshner R L, Olliger A, Simpas J B et al., 2003. OH and HO₂ Chemistry in the urban atmosphere of New York City. *Atmospheric Environment*, 37(26): 3639–3651.
- Sadanaga Y, Yoshino A, Kato S, Kajii Y, 2005. Measurements of OH reactivity and photochemical ozone production in the urban atmosphere. *Environmental Science and Technology*, 39(22): 8847–8852.
- Sadanaga Y, Yoshino A, Watanabe K, Yoshioka A, Wakazono Y, Kanaya Y et al., 2004. Development of a measurement system of OH reactivity in the atmosphere by using a laser-induced pump and probe technique. *Review of Scientific Instruments*, 75(8): 2648–2655.
- Schlosser E, Brauers T, Dorn H P, Fuchs H, Häsel R, Hofzumahaus A et al., 2009. Technical Note: Formal blind intercomparison of OH measurements: results from the international campaign HO_xComp. *Atmospheric Chemistry and Physics*, 9(20): 7923–7948.
- Sinha V, Williams J, Crowley J N, Lelieveld J, 2008. The Comparative Reactivity Method – a new tool to measure total OH Reactivity in ambient air. *Atmospheric Chemistry and Physics*, 8(8): 2213–2227.
- Whalley L K, Edwards P M, Furneaux K L, Goddard A, Ingham T, Evans M J et al., 2011. Quantifying the magnitude of a missing hydroxyl radical source in a tropical rainforest. *Atmospheric Chemistry and Physics Discussions*, 11(2): 5785–5809.
- Yoshino A, Sadanaga Y, Watanabe K, Kato S, Miyakawa Y, Matsumoto J et al., 2006. Measurement of total OH reactivity by laser-induced pump and probe technique—comprehensive observations in the urban atmosphere of Tokyo. *Atmospheric Environment*, 40(40): 7869–7881.